CDF note 8950

Angular Analysis of $B_S \to J/\psi\phi$ and $B^0 \to J/\psi K^*$ Decays and Measurement of $\Delta\Gamma_S$ and ϕ_S

The CDF Collaboration
URL http://www-cdf.fnal.gov
(Dated: September 14, 2007)

In a data sample of 1.7 fb^{-1} we select 2500 $B_s \to J/\psi\phi$ decays. With a maximum likelihood fit in mass, lifetime and angular space we extract the mean lifetime $c\tau_s$ and the decay rate difference $\Delta\Gamma_s$ between the two B_s mass eigenstates assuming no CP-violation:

$$\begin{aligned} c\tau_s &= 456 \pm 13 \text{ (stat.)} \pm 7 \text{ (syst.) } \mu\text{m} \\ \Delta\Gamma_s &= 0.076^{+0.059}_{-0.063} \text{ (stat.)} \pm 0.006 \text{ (syst.) ps}^{-1} \end{aligned}$$

Our fit result with floating CP-violating phase ϕ_s shows no evidence for CP violation.

We also report the measurement of amplitudes and phases of $B^0 \to J/\psi K^*$ decays using 7800 B^0 mesons in 1.3 fb^{-1} of data.

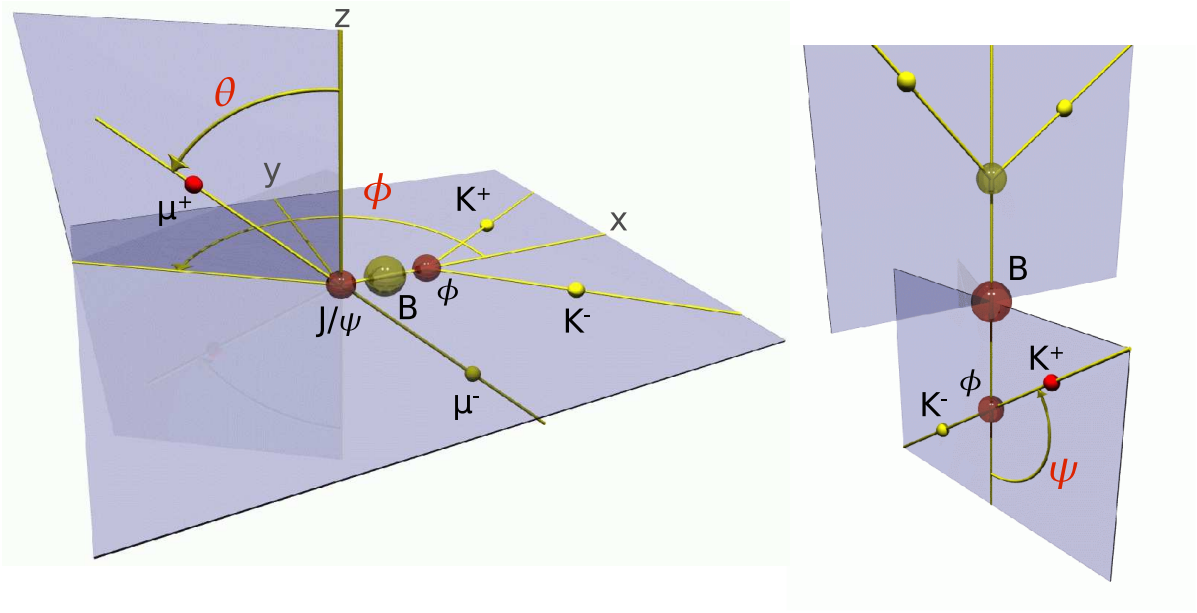

FIG. 1: Definition of transversity angles θ, ϕ and ψ.

I. INTRODUCTION

In the B_s-$\bar{B}_s$ meson system the flavor eigenstates are not the same as the mass eigenstates. The mass difference between the heavy and light mass eigenstate, B_{sH} and B_{sL}, determines the frequency of the oscillation of the B_s mesons. This quantity is known precisely since last year[1] and its measurement reduced the uncertainty on the CKM triangle significantly.

Two other quantities which determine the time evolution of B_s mesons are the decay rates Γ_H and Γ_L of the two mass eigenstates. The difference $\Delta\Gamma = \Gamma_L - \Gamma_H$ was measured first by CDF[2] and recently with higher precision by DØ[3].

If the difference $\Delta\Gamma$ is larger than a few percent of the mean decay rate $\Gamma = (\Gamma_L + \Gamma_H)/2$ a time dependent analysis of B_s decays without flavor tagging becomes sensitive to a further quantity, the CP violating phase ϕ_s. This phase describes the mixing induced CP violation and is related to the angle β_s in the nearly degenerated unitarity triangle obtained from the multiplication of the second and third column of the CKM matrix. The standard model expectation value for ϕ_s is very small[4]. Therefore a measurement of the phase which deviates significantly from zero would indicate new physics.

To determine $\Delta\Gamma$ the lifetime distribution of B_s decays is measured. Because it is very challenging to distinguish the two components of the lifetime distribution additional information is needed to separate the light and heavy mass eigenstates. Therefore we exploit the fact that in case of no CP violation ($\phi_s = 0$) the two mass eigenstates have well-defined and opposite CP parity. B_{sH} is CP odd and B_{sL} is CP even.

A decay mode that allows to measure both lifetimes is $B_s \to J/\psi\phi$ with $J/\psi \to \mu^+\mu^-$ and $\phi \to K^+K^-$ which is a composition of CP even and odd states. Because the B_s is a pseudo scalar and J/ψ and ϕ are vector mesons, the orbital angular momentum between the two decay products can have the values 0, 1 or 2. S- and D-wave decays are CP even, P-wave decays are CP odd. Consequently, the two CP eigenstates can be separated by their different angular distributions of the decay products.

The angles used in this analysis are defined in the transversity basis illustrated in Figure 1. θ and ϕ are the polar and azimuthal angle of the μ^+ in the rest frame of the J/ψ where the x-axis is defined by the direction of the B_s and the xy-plane by the $\phi \to K^+K^-$ decay plane. ψ is the helicity angle of the K^+ in the ϕ rest frame with respect to the negative B_s flight direction.

The decay $B^0 \to J/\psi K^*$ is a pseudo scalar to vector-vector decay like $B_s \to J/\psi\phi$. So the same method for the decomposition of S-, P- and D-wave can be applied. This is not only a valuable cross-check of the angular analysis technique, but a measurement with a precision competitive to the results from the B factories[5, 6].

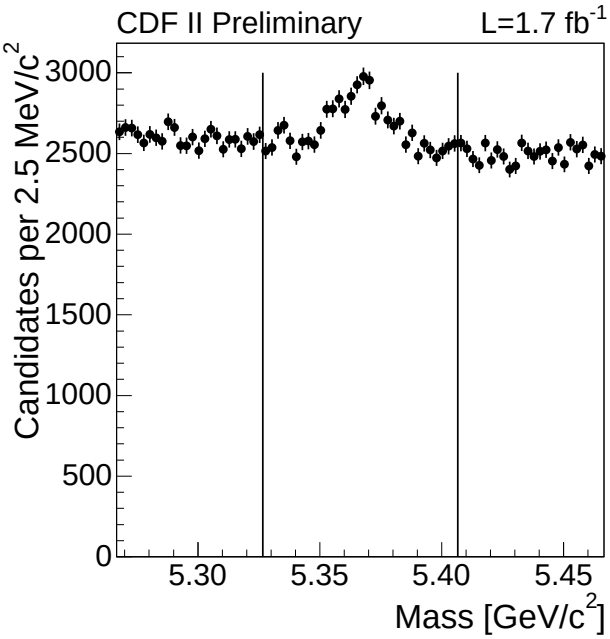

FIG. 2: Invariant mass distribution after soft precuts. The vertical lines indicate the left and right sideband mass region.

II. DATA SAMPLE AND SELECTION

For the B_s analysis we use a data sample of 1.7 fb^{-1} selected by the dimuon trigger. The tracks are reconstructed in the drift chamber COT and the silicon trackers ISL, SVXII and L00. J/ψ candidates are reconstructed from oppositely charged tracks with a transverse momentum p_T of the least 1.5 GeV/c and a matching track segment in the muon chambers CMU ($|y| < 0.6$) or CMX ($0.6 < |y| < 1$). The invariant mass of the muon candidate pair fitted to a common vertex has to be within a window of ± 80 MeV/c^2 around the world average J/ψ mass[7]. Pairs of oppositely charged tracks with $p_T > 0.4$ GeV/c are considered as ϕ candidates if the combined momentum has a transverse component above 1 GeV/c and the invariant mass is consistent with the ϕ mass within 100 MeV/c^2. J/ψ and ϕ candidates are combined in a vertex fit of all decay particles to a B_s candidate which is required to have $p_T > 4$ GeV/c.

The invariant mass distribution of the B_s candidates after this preselection is shown in Figure 2. To improve the signal selection we train a neural network on the separation of B_s decays from combinatorial background. The signal patterns are obtained from simulated B_s decays. The background events for the network training are taken from the B_s mass sidebands indicated in figure 2. As input variables we use kinematic quantities, vertex fit qualities and particle identification information obtained from the time-of-flight detector, the energy loss measurement in the drift chamber and the muon system.

Figure 3 (left) illustrates that the neural network can separate signal and background events very well. For an optimally trained network the purity of signal events has to equal to the network output scaled to [0,1]. This is checked in the right plot of Figure 3. The good agreement of the network output distribution in data and simulation is demonstrated in Figure 4 (left). For the final selection we choose a cut on the network output that maximizes the significance $S/\sqrt{S+B}$ (see Figure 4 right) where S (B) is the number of signal (background) events in a ± 20 MeV/c^2 window around the B_s mass peak position. The selected sample contains 2506 ± 51 $B_s \to J/\psi\phi$ decays.

A similar reconstruction and selection procedure is used for $B^0 \to J/\psi K^*$. The K^{*0} reconstructed via the decay to $K^+\pi^-$ is required to have a transverse momentum of at least 2 GeV/c and an invariant mass within a window of ± 80 MeV/c^2 around the world average K^* mass. Again the selection is optimized with a neural network. Figure 5 shows the good agreement of the network output distribution in data and simulation.

A peculiarity of the $B^0 \to J/\psi K^*$ decay which is no issue for the B_s analysis is the possibility that the kaon and pion hypotheses are wrongly assigned to the K^* daughter particles. This swapped assignment leads to misreconstructed masses and angles. To suppress these events we train a neural network on the identification of swapped versus non-swapped B^0 candidates. Simulated events, once reconstructed with the right, once with the swapped assignment, are used for the training. Kinematic and particle identification variables provide the network input. With a cut on

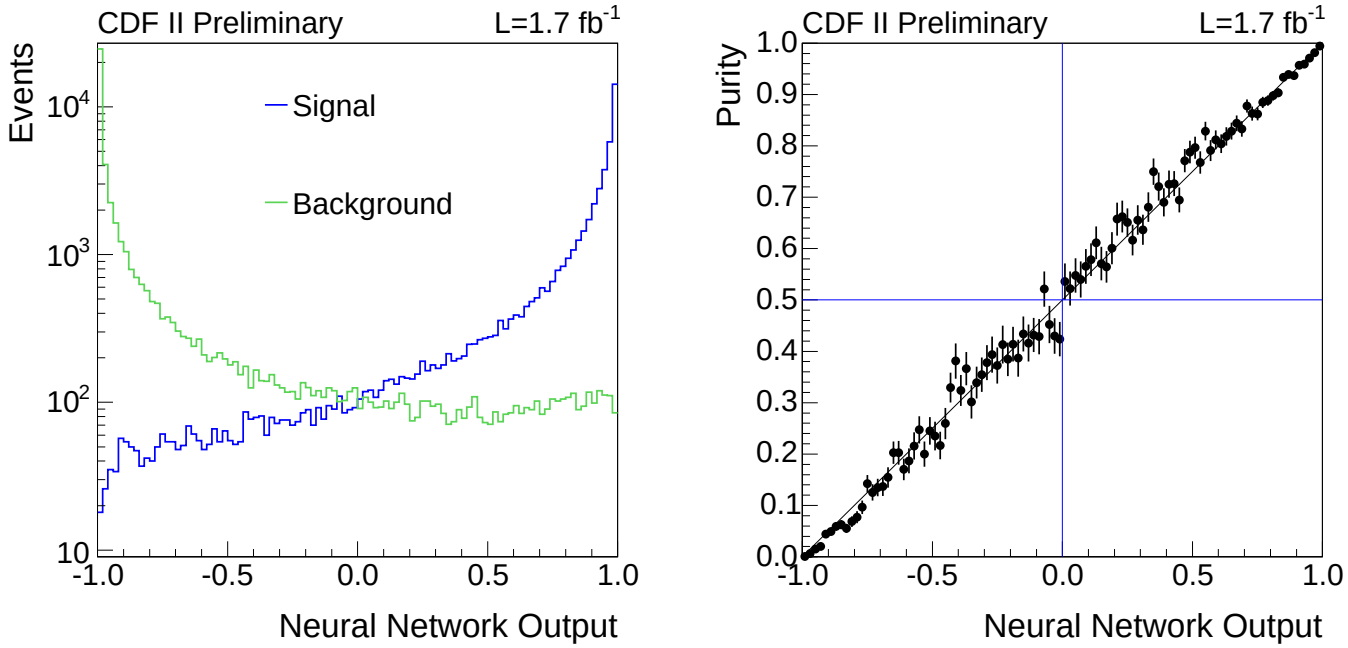

FIG. 3: Left: Network output for B_s signal and background events. Right: Purity (signal over signal plus background events) as a function of the network output.

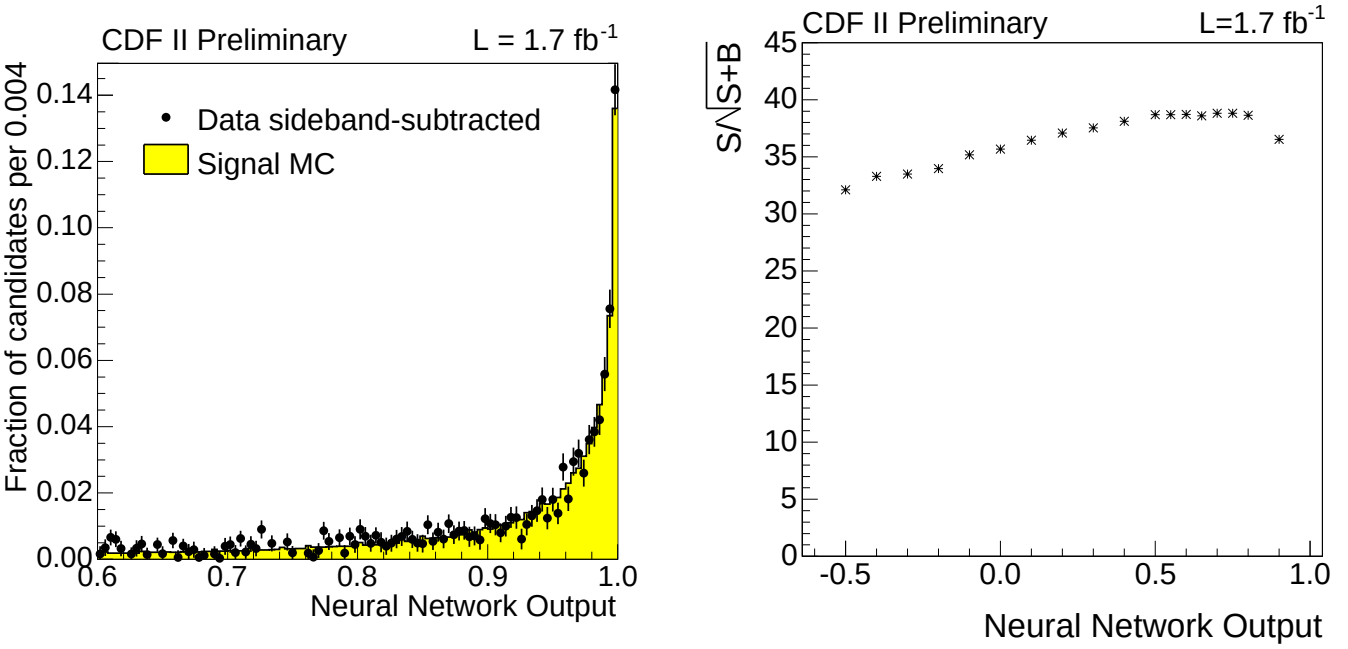

FIG. 4: Left: Comparison of the network output distribution between sideband-subtracted B_s data and simulation. Right: Significance $S/\sqrt{S+B}$ as a function of the cut on the selection network output.

the network output the fraction of events with swapped particle assignment is reduced to $\sim 0.5\%$ as estimated from simulation while keeping about half the signal events.

After swap suppression 7800 $B^0 \to J/\psi K^*$ decays remain in a data sample of 1.3 fb^{-1}.

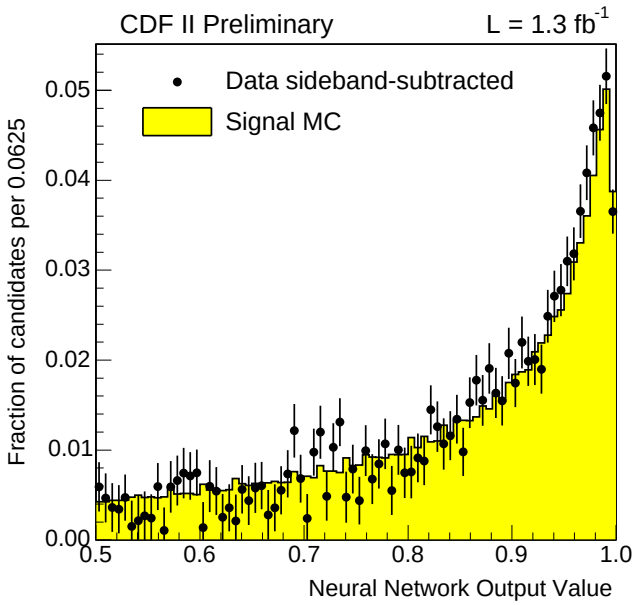

FIG. 5: Comparison of the network output distribution between sideband-subtracted B^0 data and simulation

III. MASS, LIFETIME AND ANGLE FIT

To extract the parameters of interest we perform a maximum likelihood fit in mass, lifetime and angular space.

We use empirical models for the probability density functions of the background. The mass PDF is parametrized by two first order polynomials, one for the prompt and one for the non-prompt background events. The lifetime distribution is described by a prompt component plus a negative and a positive exponential for mismeasured events plus an exponential for long lived particles. All lifetime components are convoluted with a Gaussian to account for the event-by-event lifetime resolution. For the angular PDF we use the product of polynomials in $\cos^2\theta$, $\cos 2\phi$ and $\cos\psi$. We also included terms with correlations between the three angles, but they turn out to be negligible. The angular distributions of prompt and non-prompt background events are the same within uncertainties, so we do not separate them in the likelihood function.

The mass distribution of the signal is described by the sum of two Gaussians. The lifetime and the angles $\vec{\omega} = (\cos\theta, \phi, \cos\psi)$ are correlated for B_s signal events. The distribution without acceptance effects is given by:

$$\begin{aligned}\frac{d^4P(\vec{\omega},t)}{d\vec{\omega}dt} \propto\ & |A_0|^2 f_1(\vec{\omega})\mathcal{T}_+ + |A_{||}|^2 f_2(\vec{\omega})\mathcal{T}_+ \\ +\ & |A_\perp|^2 f_3(\vec{\omega})\mathcal{T}_- + |A_0||A_{||}| f_5(\vec{\omega})\cos(\delta_{||})\mathcal{T}_+ \\ +\ & |A_{||}||A_\perp| f_4(\vec{\omega})\cos(\delta_\perp - \delta_{||})\sin\phi_s(e^{-\Gamma_H t} - e^{-\Gamma_L t})/2 \\ +\ & |A_0||A_\perp| f_6(\vec{\omega})\cos(\delta_\perp)\sin\phi_s(e^{-\Gamma_H t} - e^{-\Gamma_L t})/2 \end{aligned} \quad (1)$$

where

$$\begin{aligned}
\mathcal{T}_{\pm} &= ((1 \pm \cos\phi_s)e^{-\Gamma_L t} + (1 \mp \cos\phi_s)e^{-\Gamma_H t})/2 \\
f_1(\vec{\omega}) &= \frac{9}{32\pi} 2\cos^2\psi(1 - \sin^2\theta\cos^2\phi) \\
f_2(\vec{\omega}) &= \frac{9}{32\pi} \sin^2\psi(1 - \sin^2\theta\sin^2\phi) \\
f_3(\vec{\omega}) &= \frac{9}{32\pi} \sin^2\psi\sin^2\theta \\
f_4(\vec{\omega}) &= -\frac{9}{32\pi} \sin^2\psi\sin 2\theta\sin\phi \\
f_5(\vec{\omega}) &= \frac{9}{32\pi}\frac{1}{\sqrt{2}} \sin 2\psi\sin^2\theta\sin 2\phi \\
f_6(\vec{\omega}) &= \frac{9}{32\pi}\frac{1}{\sqrt{2}} \sin 2\psi\sin 2\theta\cos\phi
\end{aligned}$$

A_0, $A_\perp$ and $A_{||}$ are the amplitudes of the three angular components at $t = 0$. $\delta_\perp$ and $\delta_{||}$ are relative phases between them. In case of no CP violation ϕ_s is zero so that the last two terms of equation (1) vanish.

Note that the lifetime-angle distribution is invariant under the transformations

$$\begin{aligned}
\phi_s \to -\phi_s, \quad \delta_\perp \to \delta_\perp + \pi \quad \text{and} \\
\Delta\Gamma \to -\Delta\Gamma, \quad \phi_s \to \phi_s + \pi
\end{aligned} \tag{2}$$

Because of this four fold ambiguity this measurement is insensitive to the sign of ϕ_s and $\Delta\Gamma$.

For B^0 the lifetime difference is assumed to be zero so that $\frac{d^4P(\vec{\omega},t)}{d\vec{\omega}dt}$ factorizes into an exponential for the lifetime and the following angular distribution:

$$\begin{aligned}
\frac{d^3P(\vec{\omega})}{d\vec{\omega}} &\propto g_P(\vec{\omega}) \\
&= |A_0|^2 f_1(\vec{\omega}) + |A_{||}|^2 f_2(\vec{\omega}) + |A_\perp|^2 f_3(\vec{\omega}) \\
&+ |A_0||A_{||}| f_5(\vec{\omega})\cos(\delta_{||}) \\
&\pm |A_{||}||A_\perp| f_4(\vec{\omega})\sin(\delta_\perp - \delta_{||}) \\
&\pm |A_0||A_\perp| f_6(\vec{\omega})\sin(\delta_\perp)
\end{aligned} \tag{3}$$

where the sign of the last two terms is given by the charge of the kaon from the K^* decay.

As shown in [8] there can be a sizeable effect from interference of non-resonant S-wave $K\pi$ decays to the broad P-wave K^* decay. This is taken into account by introducing an absolute amplitude $|A_S|$ and a relative phase δ_S for the S-wave $K\pi$ component:

$$\begin{aligned}
g_{S+P}(\vec{\omega},\lambda) &= \cos^2\lambda \cdot g_P(\vec{\omega}) + \sin^2\lambda \cdot f_7(\vec{\omega}) \\
&+ \frac{1}{2}\sin 2\lambda \cdot \big[f_8(\vec{\omega})\cos(\delta_{||} - \delta_S)|A_{||}| \\
&+ f_9(\vec{\omega})\sin(\delta_\perp - \delta_S)|A_\perp| + f_{10}(\vec{\omega})\cos(\delta_S)|A_0| \big]
\end{aligned} \tag{4}$$

with

$$\begin{aligned}
f_7(\vec{\omega}) &= \frac{3}{32\pi} 2\left[1 - \sin^2\theta\cos^2\phi\right] \\
f_8(\vec{\omega}) &= -\frac{3}{32\pi}\sqrt{6}\sin\psi\sin^2\theta\sin 2\phi \\
f_9(\vec{\omega}) &= \frac{3}{32\pi}\sqrt{6}\sin\psi\sin 2\theta\cos\phi \\
f_{10}(\vec{\omega}) &= \frac{3}{32\pi} 4\sqrt{3}\cos\psi\left[1 - \sin^2\theta\cos^2\phi\right] \\
\cos\lambda &= \frac{A_P}{\sqrt{A_P^2 + |A_S|^2}} \\
\sin\lambda &= \frac{|A_S|}{\sqrt{A_P^2 + |A_S|^2}}
\end{aligned}$$

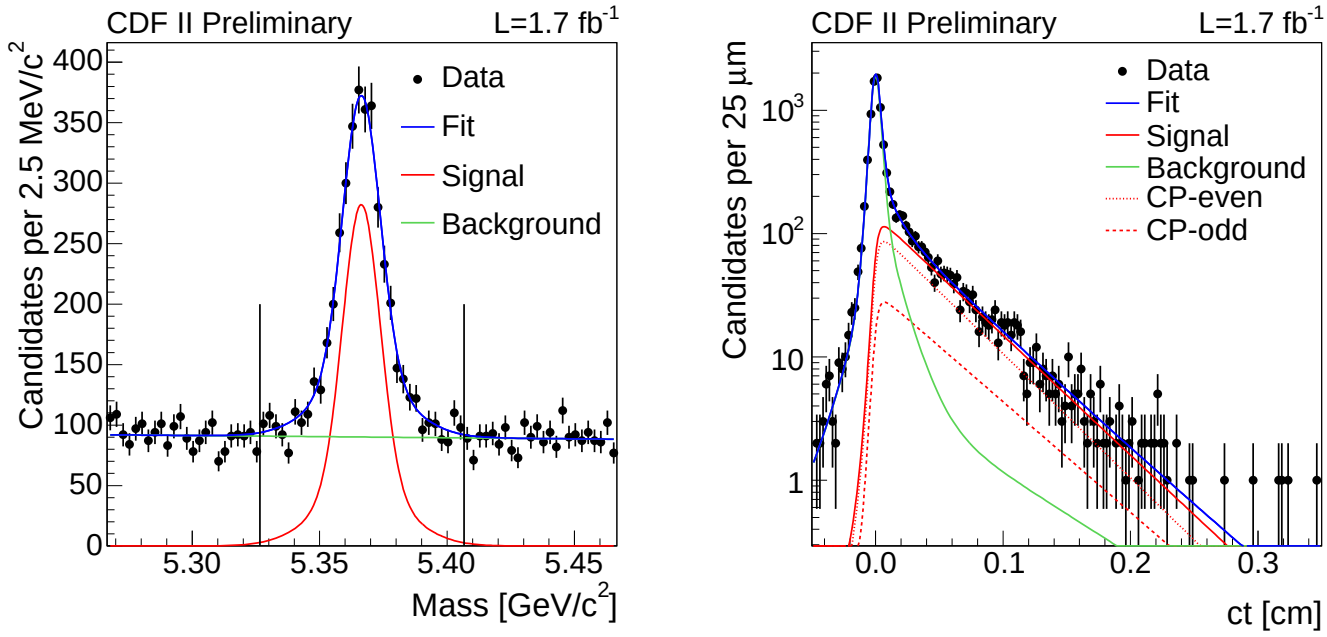

FIG. 6: Mass and lifetime projections of the B_s fit result.

Like for background the signal lifetime terms are convoluted with a Gaussian resolution function. To account for differences in the lifetime uncertainty distribution between signal and background the lifetime uncertainty PDF is included in the likelihood for both components. It is derived from sideband-subtracted signal events and sideband events, respectively.

The angular distributions described in equations (1) and (3) are modified by the detector and trigger acceptance and the selection cuts. This is taken into account by a relative differential acceptance function $A(\vec{\omega})$ derived from simulated $B_s \to J/\psi\phi$ and $B^0 \to J/\psi K^*$ decays, respectively, with a flat angular distribution. To get the right admixture of triggers the simulated events are reweighted in trigger classes defined by the muon detector component and the transverse momentum of the muons. Small differences in the p_T spectrum of the B_s are also corrected via reweigthing. $A(\vec{\omega})$ is described by a 3D histogram with 20 bins in each of the angles. This allows to calculate the normalization analytically.

The projections of the B_s fit result with ϕ_s set to zero are shown in Figures 6 and 7. Good agreement with data is observed. The analog plots for the B^0 fit are shown in figures 8 and 9. Figure 10 demonstrates the improvement of the fit result for the most sensitive angular distribution $\cos\psi$ achieved by the inclusion of the $K\pi$ S-wave interference terms in the angular model.

IV. SYSTEMATIC UNCERTAINTIES

We considered several systematic uncertainties that could affect the result. The effects are estimated from pseudo experiments generated with a different model than the one used in the fit.

The systematic uncertainty due to the model for the angular distribution of the background is determined from a fit with lower order polynomials for the background PDF than used in the pseudo experiment generation. For the estimation of the influence of the mass model we fitted with a single instead of a double Gaussian. The lifetime resolution model dependence was studied by adding exponential tails in the generated resolution function.

$B^0 \to J/\psi K^*$ decays can be misreconstructed and selected as B_s candidates. The fraction, estimated from fragmentation and branching ratio and selection efficiencies, is 2.5%. Their influence on the B_s result was evaluated by adding 3% of B^0 to the generated events.

The B^0 fit result can be affected by the remaining fraction of $B^0 \to J/\psi K^*$ events with swapped $K\pi$ particle assignment. This effect was estimated by adding twice the expected fraction of swapped events to the pseudo experiments. The influence of the neglected mass dependence of the $K\pi$ S-wave interference terms on the B^0 fit result was evaluated by fitting without these terms. Another systematic effect that we only observe for B^0 is due to the different

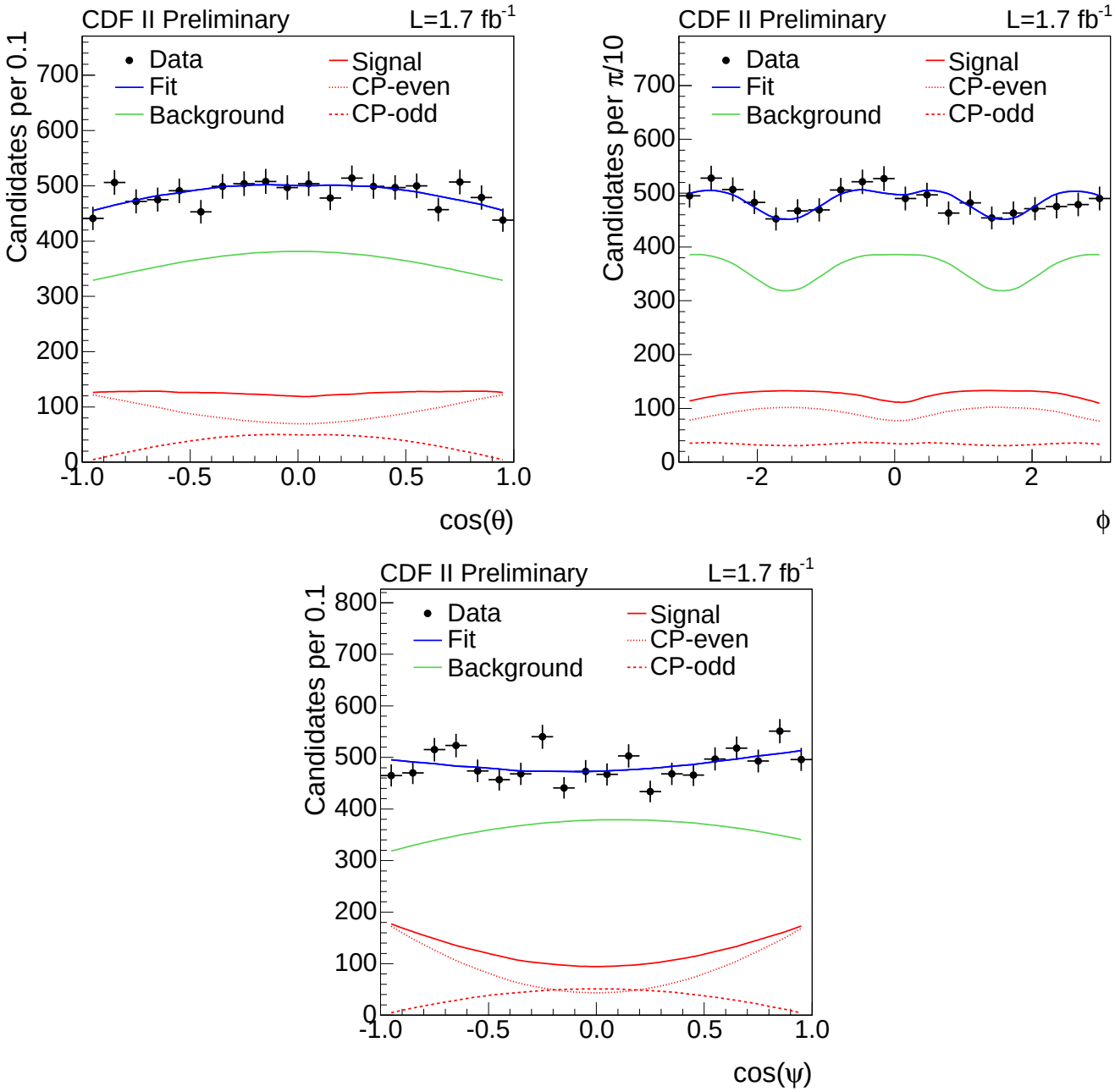

FIG. 7: Angular projections of the B_s fit result.

lifetime uncertainty PDFs for signal and background. If they are not considered in the fit the resulting parameters shift more than expected by pseudo experiments so that we assign half the shift as systematic uncertainty.

The systematic uncertainty due to the acceptance description was determined by using a parametrized function instead of a histogram for the pseudo experiment generation and by using an alternative reweighting procedure for the Monte-Carlo. Finally the effect of a silicon detector misalignment was considered.

The largest systematic uncertainty for $\Delta\Gamma$ is caused by the B^0 cross feed, however all systematic errors are much smaller than the statistical one. The largest contribution to the systematic uncertainty of the mean lifetime is the lifetime resolution model and the silicon detector alignment.

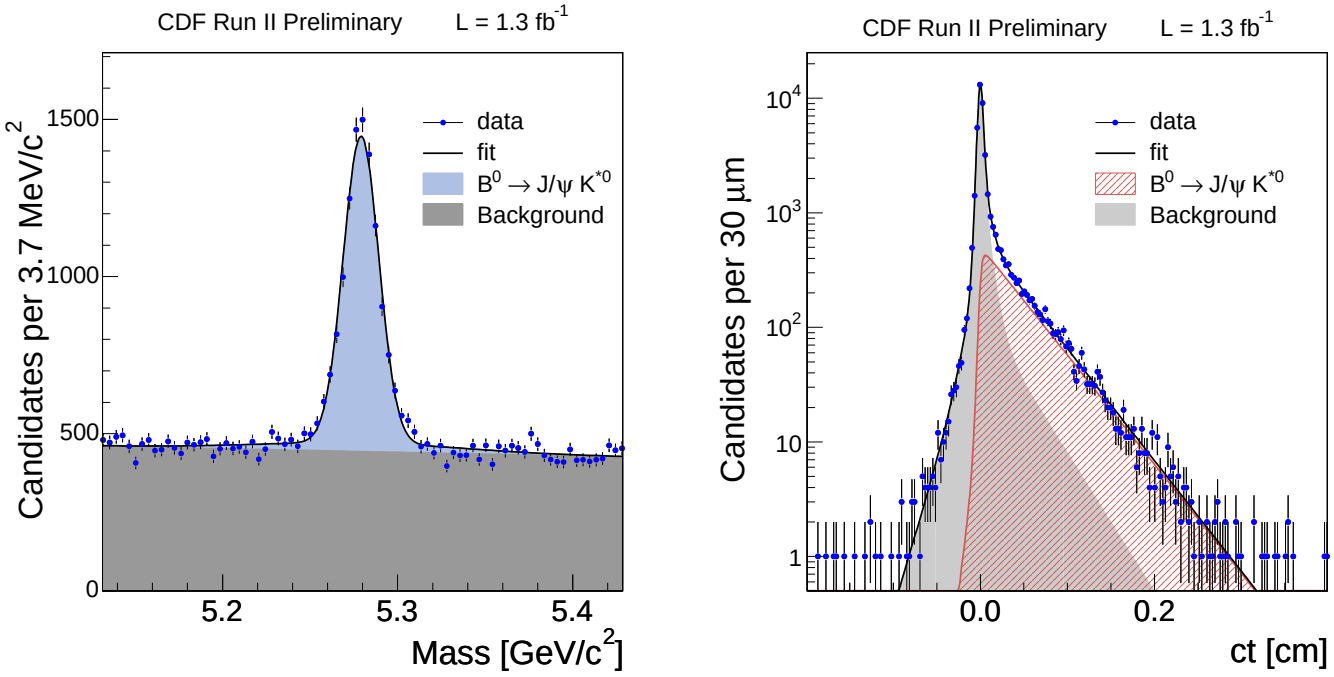

FIG. 8: Mass and lifetime projections of the B^0 fit result.

V. CONFIDENCE REGION

In the B_s fit with floating ϕ_s we observe in pseudo experiments for low values of $\Delta\Gamma$ and ϕ_s a bias towards higher values. This can be understood by looking at equation (1). If ϕ_s gets zero the last two terms vanish and the phase $\delta_\perp$ becomes undetermined. This corresponds to an effective loss of a degree of freedom. The fit can not improve the description of the data any more by varying $\delta_\perp$. The situation is similar if $\Delta\Gamma$ approaches zero. Again the last two terms of equation (1) vanish and ϕ_s and $\delta_\perp$ become undetermined.

Because of this bias we don't quote a point estimate, but use a frequentist method that takes into account the bias to calculate a p-value and a confidence region in the $\Delta\Gamma$-ϕ_s plane. The p-value quantifies the probability to get the observed fit result for given true values of $\Delta\Gamma$ and ϕ_s. It is determined from the ratio of likelihoods of a fit with all parameters floating to a fit with $\Delta\Gamma$ and ϕ_s fixed to the assumed true values as suggested by Feldman and Cousins[9]:

$$R(\Delta\Gamma, \phi_s) \;=\; \log \frac{\mathcal{L}(\hat{\Delta\Gamma}, \hat{\phi_s}, \hat{\theta})}{\mathcal{L}(\Delta\Gamma, \phi_s, \hat{\theta}')} \tag{5}$$

Here θ denotes all other fit parameters and the hat indicates the values of parameters that minimize the likelihood $\mathcal{L}$.

The distribution of R for assumed true values of $\Delta\Gamma$ and ϕ_s is determined from pseudo experiments. They are generated with the parameters θ set to the values obtained from a fit to data with $\Delta\Gamma$ and ϕ_s fixed to the tested values. We checked that this procedure known as plug-in method does not lead to a significant over- or undercoverage.

The p-value is determined by the fraction of pseudo experiments with a R value higher than the value obtained from data. The region with a confidence level of α is defined by the $\Delta\Gamma$-ϕ_s pairs with a p-value above $1-\alpha$. Systematic uncertainties are not accounted for in this calculation, but our studies indicate that their effect on the p-value and the confidence region is small.

VI. RESULT

From the maximum likelihood fit in mass, lifetime and angular space to $B_s \to J/\psi\phi$ candidates selected with a neural network we obtain under the assumption of no CP-violation the following values with the systematic uncertainties

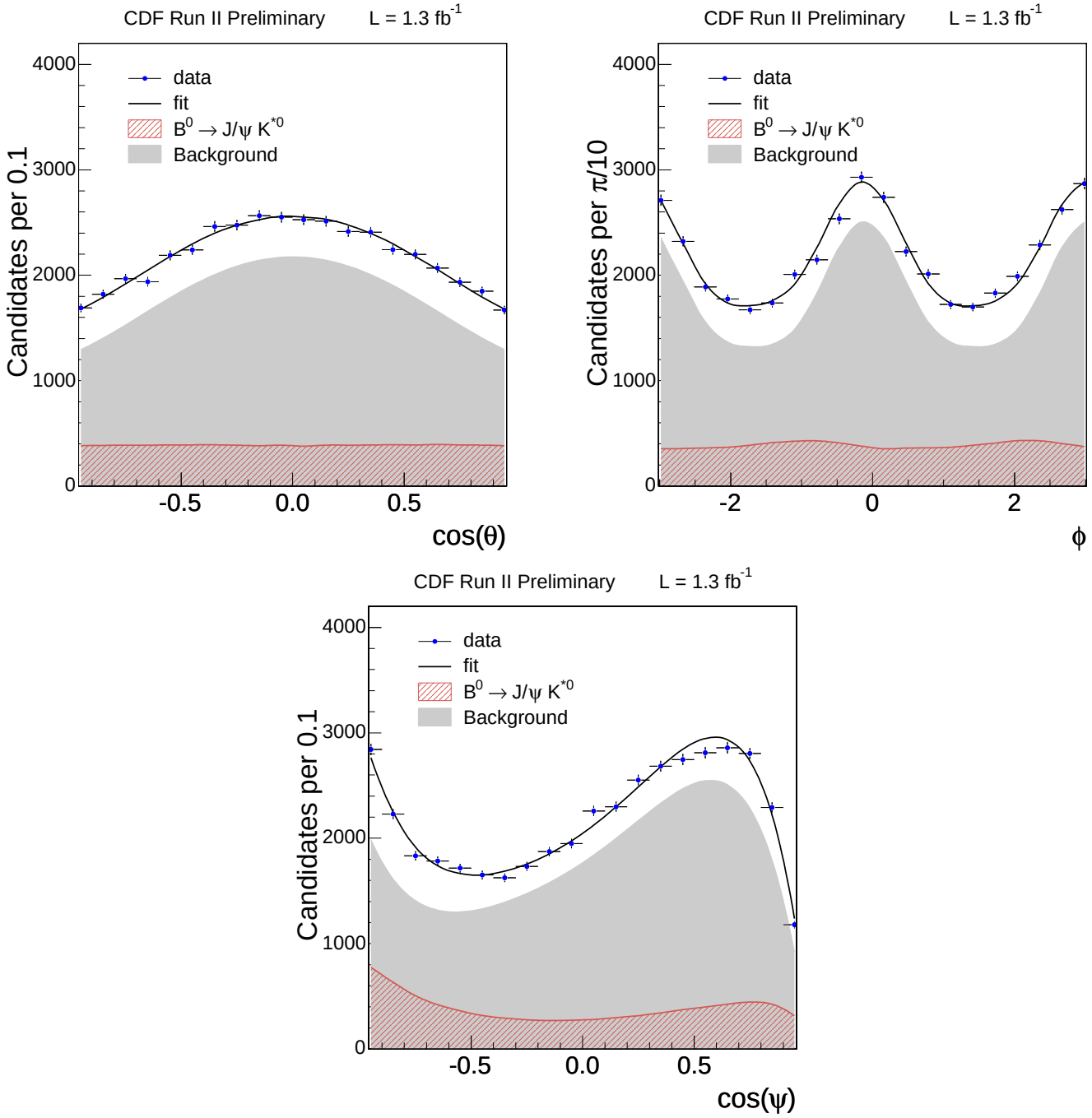

FIG. 9: Angular projections of the B^0 fit result.

discussed above:

$$
\begin{aligned}
c\tau_s &= 456 \pm 13 \pm 7\ \mu\text{m} \\
\Delta\Gamma &= 0.076^{+0.059}_{-0.063} \pm 0.006\ \text{ps}^{-1} \\
|A_0|^2 &= 0.530 \pm 0.021 \pm 0.007 \\
|A_{||}|^2 &= 0.230 \pm 0.027 \pm 0.009
\end{aligned}
$$

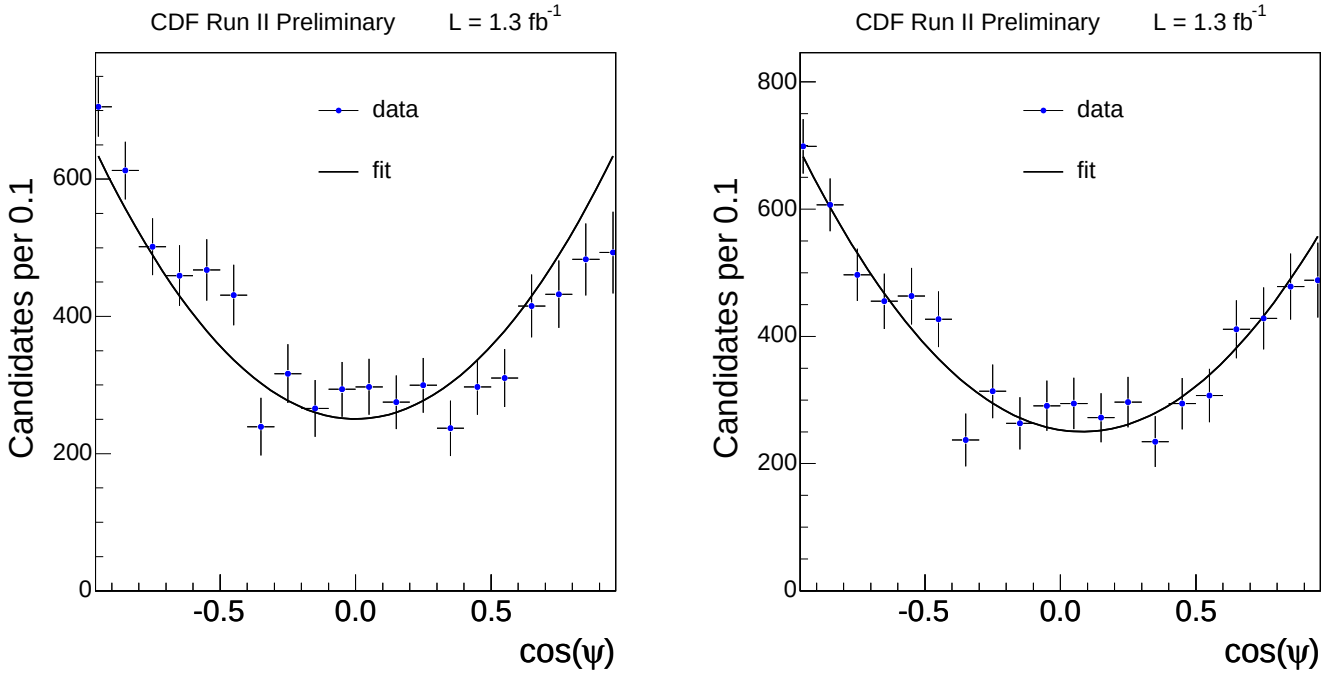

FIG. 10: $\cos\psi$ fit projections for sideband subtracted and acceptance correted data without (left) and with (right) $K\pi$ S-wave component.

The first is the statistical and the second one the systematic uncertainty. $\tau_s = 1/\Gamma$ is the mean B_s lifetime. This is currently the most precise measurement of this quantity. Likelihood scans for $c\tau_s$, $\Delta\Gamma$ and $\delta_{||}$ are shown in Figure 11. Since the likelihood scan for the strong phase $\delta_{||}$ has a non-parabolic shape we don't quote a point estimate for this quantity.

τ_s is expected to be equal to the B^0 lifetime within 1%. Using this as a constraint we obtain

$$\begin{aligned} c\tau_s &= 458 \pm 5 \pm 7\ \mu\text{m} \\ \Delta\Gamma &= 0.081 \pm 0.050 \pm 0.006\ \text{ps}^{-1} \\ |A_0|^2 &= 0.531 \pm 0.020 \pm 0.007 \\ |A_{||}|^2 &= 0.230 \pm 0.026 \pm 0.009 \end{aligned}$$

The fit result with floating CP-vioalting phase ϕ_s is compatible with the standard model. The p-value for $\Delta\Gamma = 0.1$ ps^{-1} and $\phi_s = 0$ is 22%. The $\Delta\Gamma$ and ϕ_s values excluded at a 90% and 95% confidence level are shown in Figure 12. Our Measurement does not exclude any values of $\Delta\Gamma$ and ϕ_s that are possible in minimal flavor violating new physics scenarios[4] which change the phase ϕ_s, but do not significantly affect $b \to c\bar{c}s$ tree level dominated processes.

The angular analysis of $B^0 \to J/\psi K^*$ decays yields a result that is in good agreement and of competitive precision with the results from BaBar and Belle:

$$\begin{aligned} c\tau_d &= 456 \pm 6 \pm 6\ \mu\text{m} \\ |A_0|^2 &= 0.569 \pm 0.009 \pm 0.009 \\ |A_{||}|^2 &= 0.211 \pm 0.012 \pm 0.006 \\ \delta_{||} &= -2.96 \pm 0.08 \pm 0.03 \\ \delta_{\perp} &= 2.97 \pm 0.06 \pm 0.01 \end{aligned}$$

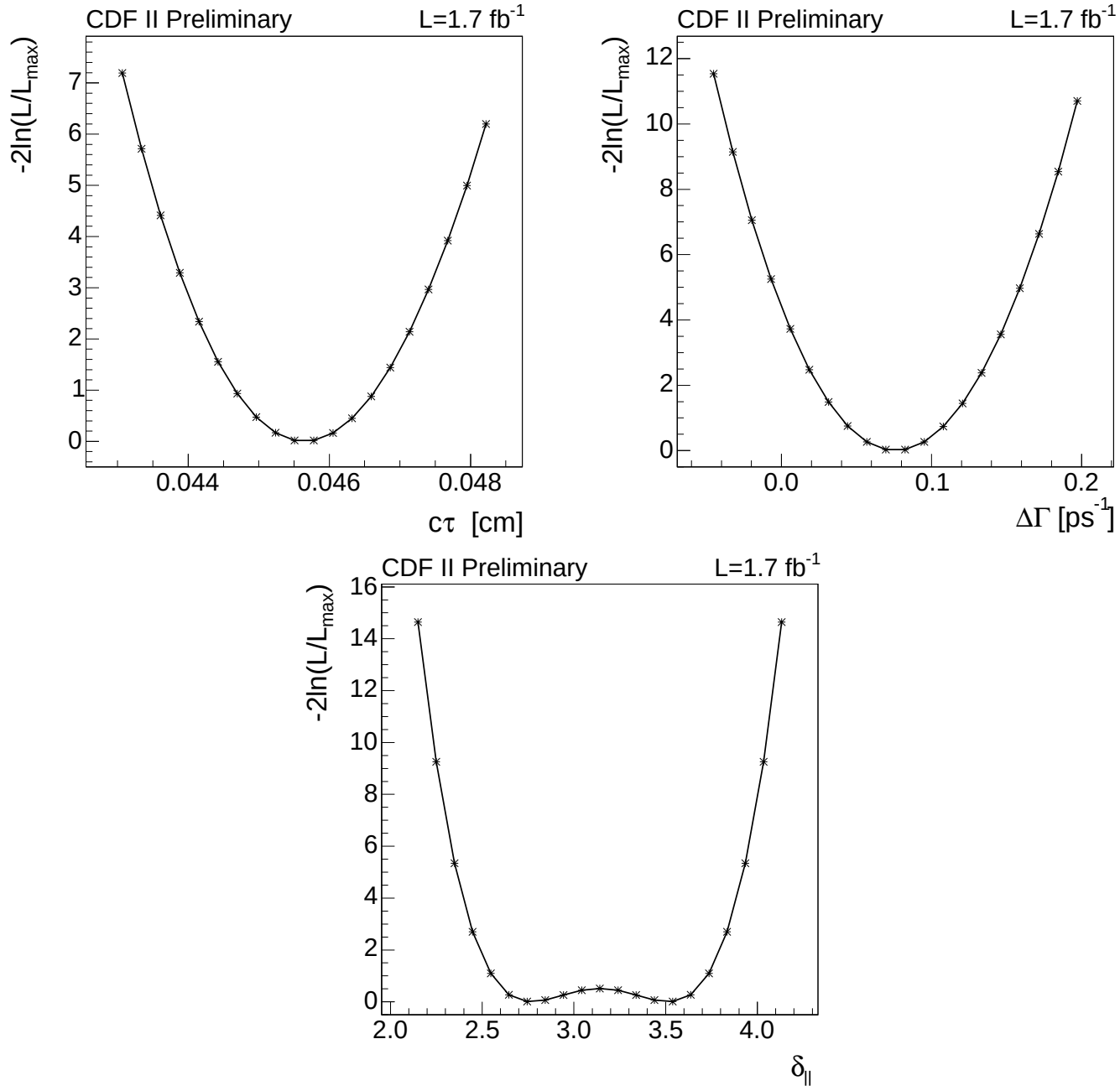

FIG. 11: Likelihood scans of $c\tau_s$, $\Delta\Gamma$ and $\delta_{||}$ for the B_s fit.

Acknowledgments

We thank the Fermilab staff and the technical staffs of the participating institutions for their vital contributions. This work was supported by the U.S. Department of Energy and National Science Foundation; the Italian Istituto Nazionale di Fisica Nucleare; the Ministry of Education, Culture, Sports, Science and Technology of Japan; the Natural Sciences and Engineering Research Council of Canada; the National Science Council of the Republic of China; the Swiss National Science Foundation; the A.P. Sloan Foundation; the Bundesministerium für Bildung und Forschung, Germany; the Korean Science and Engineering Foundation and the Korean Research Foundation; the Science and Technology Facilities Council and the Royal Society, UK; the Institut National de Physique Nucleaire et Physique des Particules/CNRS; the Russian Foundation for Basic Research; the Comisión Interministerial de Ciencia

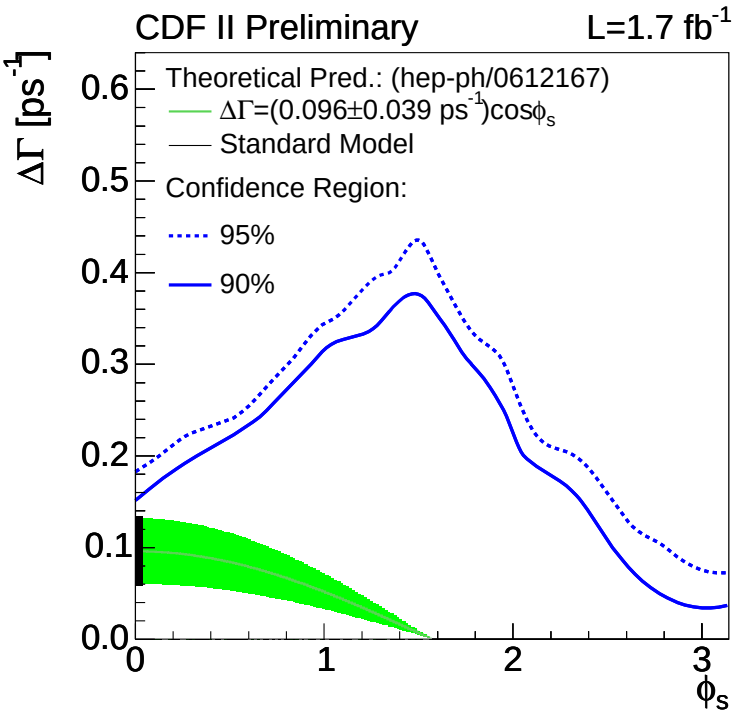

FIG. 12: 90% and 95% confidence region in the ϕ_s-$\Delta\Gamma_s$ plane. Only the first quadrant is shown. The other three quadrants can be obtained via the transformations $\phi_s \to -\phi_s$ and $\Delta\Gamma \to -\Delta\Gamma$, $\phi_s \to \phi_s + \pi$.

y Tecnología, Spain; the European Community's Human Potential Programme; the Slovak R&D Agency; and the Academy of Finland.

[1] A. Abulencia et al. Observation of B_s^0-$\bar{B}_s^0$ oscillations. *Phys. Rev. Lett.*, 97:242003, 2006.
[2] D. Acosta et al. Measurement of the lifetime difference between B_s mass eigenstates. *Phys. Rev. Lett.*, 94:101803, 2005.
[3] V. M. Abazov et al. Lifetime difference and CP-violating phase in the B_s^0 system. *Phys. Rev. Lett.*, 98:121801, 2007.
[4] Alexander Lenz and Ulrich Nierste. Theoretical update of $B_s - \bar{B}_s$ mixing. *JHEP*, 06:072, 2007.
[5] R. Itoh et al. Studies of CP violation in $B \to J/\psi K^*$ decays. *Phys. Rev. Lett.*, 95:091601, 2005.
[6] B. Aubert et al. Measurement of Decay Amplitudes of $B \to (c\bar{c})K^*$ with an Angular Analysis, for $(c\bar{c}) = J/\psi$, $\psi(2S)$ and χ_{c1}. 2007.
[7] W.-M. Yao et al. Review of Particle Physics. *Journal of Physics G*, 33:1+, 2006.
[8] B. Aubert et al. Ambiguity-free measurement of $\cos(2\beta)$: Time- integrated and time-dependent angular analyses of $B \to J/\psi K\pi$. *Phys. Rev.*, D71:032005, 2005.
[9] Gary J. Feldman and Robert D. Cousins. A unified approach to the classical statistical analysis of small signals. *Phys. Rev.*, D57:3873–3889, 1998.